Quantification of methane sources in the Barnett Shale (Texas) using the Penn State WRF-Chem-FDDA realtime modeling system

Thomas Lauvaux[1], Aijun Deng[1], Brian Gaudet[1], Colm Sweeney[2], Gaby Petron[2], Anna Karion[2], Alan Brewer[2], Mike Hardesty[2], Scott Herndon[3], Tara Yacovitch[3], Stephen Conley[4]

1: Department of Meteorology, PennState University, 2: University of Colorado – ESRL/GMD/NOAA, 3: Aerodyne Research, Inc., 4: University of California, Davis

Introduction

Methane emissions from natural gas production areas are subject to large uncertainties at regional scales. Top-down methodologies offer an integrated approach to monitor these emissions but highly depend on the quality of the atmospheric model used to relate the surface emissions to the observed atmospheric concentrations. Using continuous atmospheric measurements of in-situ methane and ethane mixing ratios from an intensive aircraft campaign over the Barnett Shale area in March 2013, we developed an atmospheric inversion system based on high resolution WRF simulations (1 km) and a Lagrangian Particle Dispersion Model (LPDM) (Uliasz, 1995) to invert for the methane sources in the area. We present here the performance of the WRF-FDDA modeling system (Deng et al., 2012) using WMO surface stations and aircraft meteorological measurements (wind, temperature, humidity) compared to the initial WRF simulation in historical mode. We evaluated the impact of the additional aircraft data assimilated in WRF-FDDA by using the concentration footprints along the different flight transects, and estimated the correlation between the locations of the footprints and the ethane-to-methane ratio of the sources. We finally discuss the modeling performance of our WRF-FDDA-LPDM system to distinguish the two major contributors to methane emissions in the area, i.e. from the urban area of Dallas-Fort Worth and from the Barnett shale gas activities.

Model description, system configuration, and evaluation

The WRF configuration for the model physics used for this study is the same as those used in Penn State NEXGEN airport forecast system (NGAFS, Deng et al. 2012), and is identical to the model physics used in Rapid Refresh (RAP) and High Resolution Rapid Refresh (HRRR) systems. This configuration includes the use of: 1) the Thompson microphysical processes, 2) the Grell 3-D ensemble scheme for cumulus parameterization on the coarse grid, 3) the Rapid Radiative Transfer Model (RRTM) for longwave atmospheric radiation, and the Dudhia scheme for shortwave atmospheric radiation, 4) the TKE-predicting Mellor-Yamada Level 2.5 turbulent closure scheme (MYJ PBL) for boundary layer turbulence parameterization, and 5) the 6-level RUC land surface model (LSM) for representation of the interaction between the land surface and the atmospheric surface layer.

The WRF modeling system also has four-dimensional data assimilation (FDDA) capabilities to allow the meteorological observations to be continuously assimilated into the model. The FDDA technique used in this study was originally developed for MM5 (Stauffer and Seaman 1994) and recently implemented into WRF (Deng et al. 2009). It has several major uses. Firstly, it can be used to create four-dimensional dynamically consistent data sets or dynamic analyses (e.g., Deng et al. 2004, Deng and Stauffer 2006, Rogers et al. 2013). Secondly, it can also be used to create improved lateral boundary conditions for process studies (e.g., Reen et al. 2006). Finally, it can be used for dynamic initialization, where the model is relaxed towards observations during a pre-forecast period to improve the initial state and the subsequent short-term forecast (e.g., Deng et al. 2012).

Configuration

The WRF model grid configuration used for this study is comprised of four grids: 9 km, 3 km and 1 km (Figure 1). The 9-km grid, with a mesh of 322x232 grid points, contains the most part of southwestern U.S. The 3-km grid, with a mesh of 202x202 grid points, contains part of Oklahoma and part of Texas. The 1-km grid, with a mesh of 202x202, only covers a small portion of northern Texas.

Fifty (50) vertical terrain-following layers are used, with the center point of the lowest model layer located ~12 m above ground level (AGL). The thickness of the layers increases gradually with height, with 27 layers below 850 hPa (~1550 m AGL). Note that WRF's vertical layers are defined based on the dry hydrostatic pressure and the height of the center point of each layer changes with time. The top of the model is set at 100 hPa. A one-way nesting strategy is used so that information from the coarse domains defines the lateral boundaries of the fine domains but no information from the fine domains feeds back to the coarse domains.

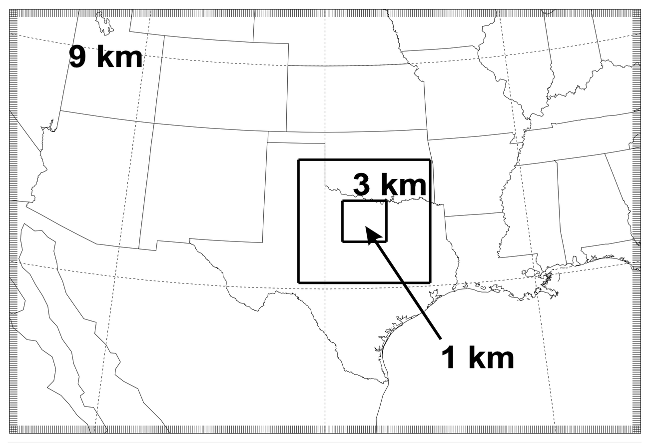

Figure 1: WRF nested *domain configuration using 9/3/1 km spatial resolutions, centered on the Barnett Shale gas*

Table 1 lists the FDDA parameters used in this application. As indicated in the table, for this application, 3D analysis nudging was applied on the 9-km grid, and observation nudging was applied on all grids with the same nudging strength. No mass fields (temperature and moisture) observations are assimilated within the WRF-predicted PBL. The meteorological observation data assimilated into the WRF system, the World Meteorological Organization (WMO) observations distributed by the National Weather Service (NWS), include both 12-hourly upper-air rawinsondes and hourly surface observations.

	Analysis nudging			Observation nudging		
	9km	3km	1km	9km	3km	1km
G (1/sec)	$3*10^{-4}$	N/A	N/A	4.10^{-4}	4.10^{-4}	4.10^{-4}
RINXY (km)	N/A	N/A	N/A	150*	100*	100*
Twindo (hr)	N/A	N/A	N/A	2**	2**	2**

** 0.67 factor for surface, 2.0 factor at 500 hPa and above*
*** 0.5 factor for surface*

Table 1: *Multiscale FDDA parameters used in* NGAFS, where G is the nudging coefficient, RINXY is the radius of influence used in obs nudging, and TWINDO is the time window used in obs *nudging.*

Evaluation

To evaluate the WRF model performance on the 1-kim grid among the three experiments, mean absolute error (MAE) statistics for temperature, wind speed, and wind direction were computed to measure the model error. Sixteen surface stations and one upper-air sounding from Fort Worth (KFWD), throughout the 48 hour period, between 12 UTC 26 March and 12 UTC 28 March 2013, were used in the meteorological evaluations. Comparison of the MAE time series of WRF-simulated surface wind speed and wind direction (temperature is not assimilated) among the three experiments indicated that the added value of assimilating surface winds is evident (e.g. Fig. 2), since the surface wind direction MAE statistics are consistently improved in the FDDA experiments. For the upper-air statistics (e.g. Fig. 3), assimilation of WMO sonde data at KFWD substantially improved the WRF solutions for all three fields, since mass fields along with winds were assimilated above the boundary layer; however, there was still more significant improvement in the wind fields, especially in wind direction (e.g., ~30 degree improvement in the lowest kilometer). Comparison between Experiment FDDA and FDDA-w-Aircraft shows that assimilating aircraft obs generally further improves the WRF simulation, but the improvement is not as significant as that of using WMO only. This is likely because the MAE is computed at the KFWD location where the KFWD sonde is assimilated.

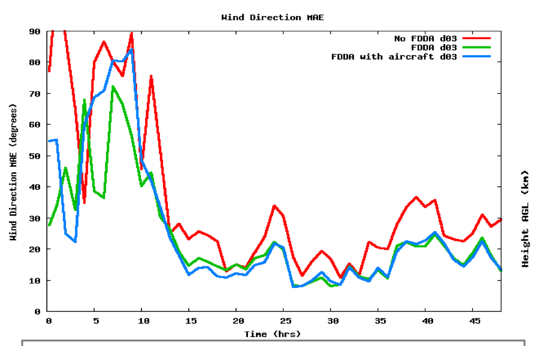

Figure 2: Mean wind direction model-data differences for WRF (in red), WRF-FDDA (in blue), WRF-FDDA-w-Aircraft (in green) from March 26 (6:00 UTC) to March 27 (24:00 UTC).

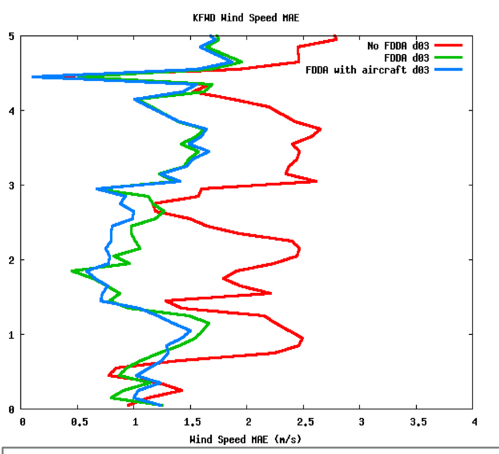

Figure 3: Profiles of the mean wind speed model-data differences for WRF (in red), WRF-FDDA (in blue), WRF-FDDA-w-Aircraft (in green) from March 27 (12:00 UTC).

Aircraft campaign

In March and April 2013, an aircraft and ground-based mobile campaign was launched with the objective of quantifying methane fluxes from the Barnett Shale natural gas production field. A Mooney TLS-20 single engine aircraft (owned and operated by Scientific Aviation) was instrumented with a CRDS $CO_2/CH_4/CO/H_2O$ (Picarro) analyzer as well as an ethane (C_2H_6) analyzer (Aerodyne). Discrete flask air samples (NOAA/ESRL) were also collected on board. All instruments drew air from outside the aircraft from dedicated inlets installed under the starboard wing. Pressure, temperature, and horizontal winds were also measured on the aircraft.

Five science flights were conducted in the Barnett region during clear weather conditions. Flight paths sampled air upwind and downwind of the gas field and the urban Dallas/Fort Worth area. The aircraft conducted two vertical profiles per flight to measure the mixing height of surface emissions. We present here the measurements for ethane (C_2H_6) and methane (CH_4) during one of the flights (March 27, 2013) with the time series (Figure 6) and the map on Figures 4 and 5.

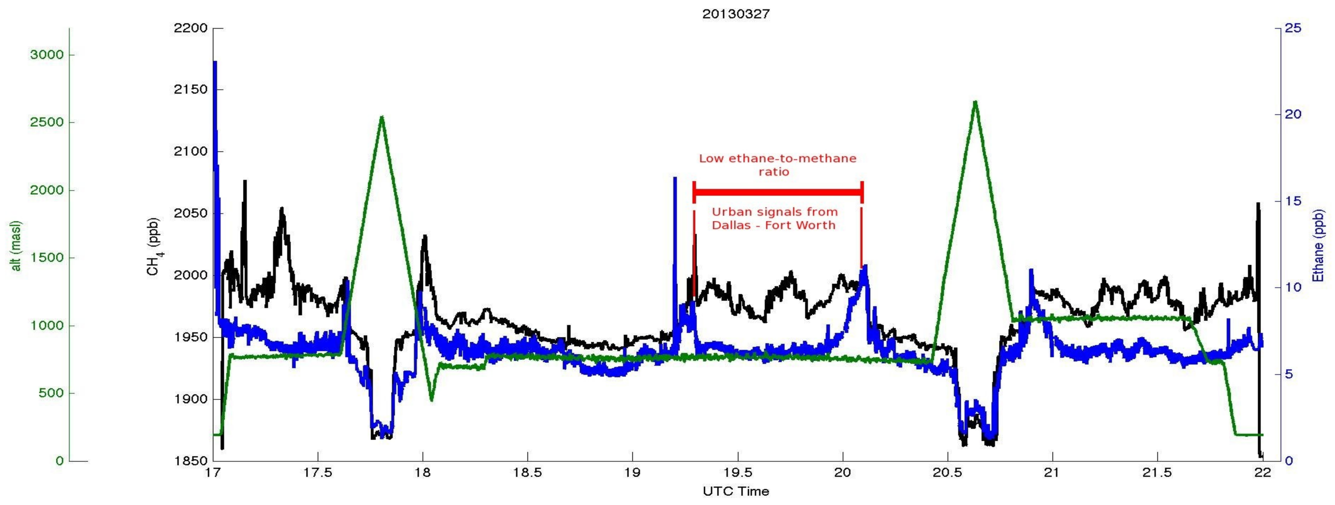

Figure 6: Time series of the observed atmospheric methane (in black) and ethane (in blue) mole fractions, and flight altitudes (in green) during the March 27, 2013 flight.

CH_4 enhancement with little C_2H_6 enhancement

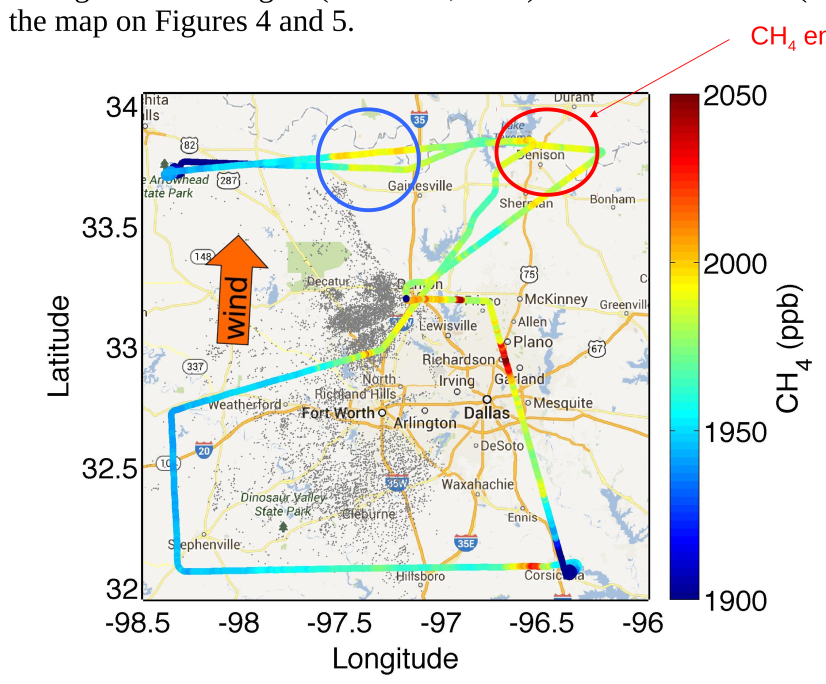

Figure 4: Map of the observed atmospheric methane (CH4) mole fractions along the flight track for March 27, 2013 (in ppb). Natural gas well locations are indicated in gray.

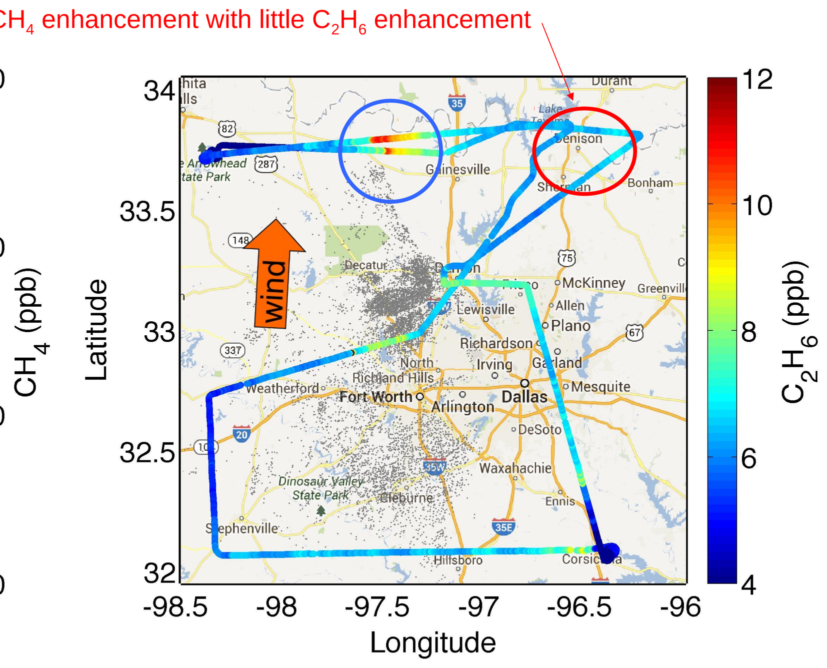

Figure 5: Map of the observed atmospheric ethane (C2H6) mole fractions along the flight track for March 27, 2013 (in ppb). Natural gas well locations are indicated in gray.

Ethane (C_2H_6) and methane (CH_4) measurements from the aircraft illustrate the presence of CH_4 enhancements that correlate with C_2H_6 enhancements (left, blue circles), as well as the locations of CH_4 enhancements with no corresponding C_2H_6 enhancements (left, red circles and above, at ~19.5 hours). Ethane is a component of raw gas, making it a good tracer for fugitive gas and oil-related emissions. CH_4 emissions from urban sources, such as landfills and wastewater treatment, have no correlated C_2H_6, which is not emitted by those sources. We selected the locations and time of the aircraft measurements with a low ethane-to-methane ratio for our WRF experiment to evaluate the performance of the model for the detection of urban emissions in the middle of the Barnett Shale gas production area. The experiment would be similar for point source detection using mesoscale modeling at high resolution.

Methane emissions: Life Cycle modeling and uncertainties

Many measurements to date have focused on CH_4 mole fraction measurements, with no quantification of emissions (e.g. Philips et al., 2012). Measurements of fugitive emissions from gas production have focused primarily on measurements at the level of individual well pads, compressors, or even individual components of the plumbing within production facilities (EPA/GRI, 1996). This work has led to the creation of emissions factors which, when combined with activity data and extrapolated from a small number of one-time field measurements to tens of thousands of continuously operating well pads, provide existing emissions estimates (cf. Table 2). This approach is prone to systematic error, as emissions are highly variable across production facilities and change over time with industry practice.

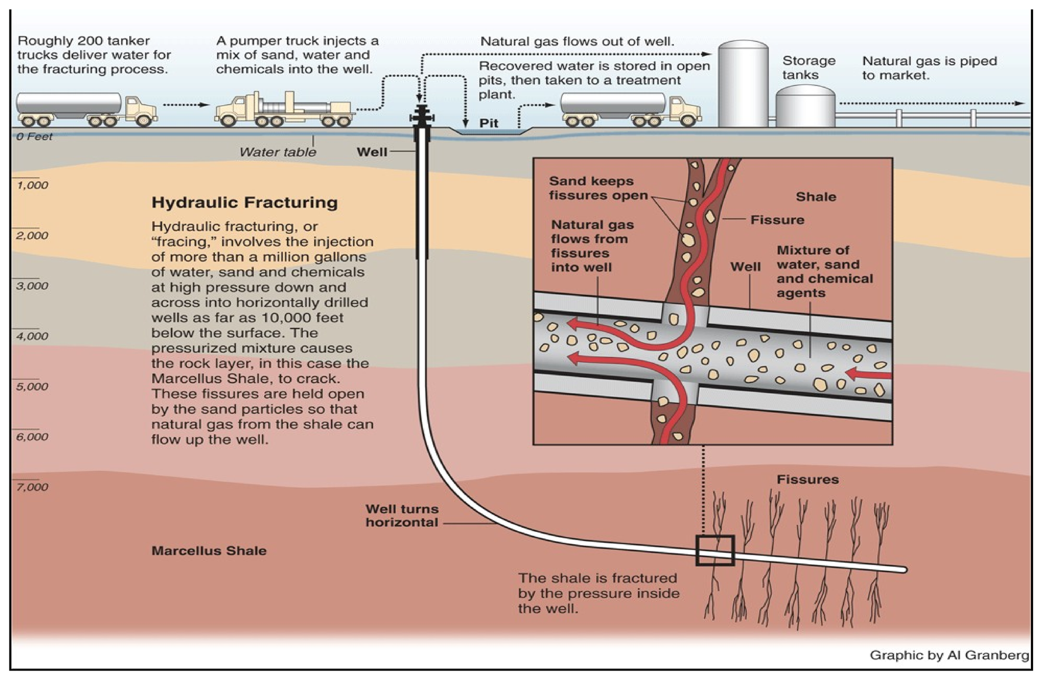

Large-area (~10⁴ km²) estimates from atmospheric measurements show great promise to address the shortcomings in existing shale gas emissions data. Aircraft missions have been used to document emissions from entire gas fields for limited periods of times (e.g., measurements over a single day). A single tower and mobile lab measurements were used in an emission ratio approach to estimate long-term emissions from drilling in the Denver-Julesburg basin of Colorado (Petron et al., 2012). This work also showed relatively large emissions (~4% of production). We propose here to use simulated mesoscale meteorological variables to compute the source-receptor relationship instead of aircraft observations and quantify the emissions from gas production activities in the Barnett Shale area.

Sources of uncertainty in Life Cycle models
(from NETL – DoE)

Data Uncertainty
– Episodic emission factors
– Formation-specific production rates
– Flaring rates (extraction and processing)
– Natural gas pipeline transport distance
Data Availability
– *Formation-specific gas compositions (including CH4, H2S, NMVOC, and water)*
– Effectiveness of green completions and workovers
– Fugitive emissions from around wellheads (between the well casing and the ground)

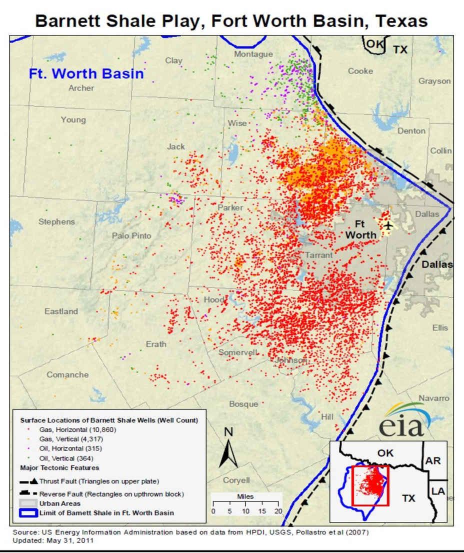

Howarth et al. (2011)	3.3 %	(mean; range = 2.2% to 4.3%)
EPA (2011)*	3.0 %	
Jiang et al. (2011)	2.0 %	
Hultman et al. (2011)	2.8 %	
Burnham et al. (2011)	1.3 %	
Stephenson et al. (2011)	0.6 %	
Cathles et al. (2012)	0.9 %	
Petron et al. (2012)	4.0 %	("best estimate;" range = 2.3 to 7.7%)

* The EPA (2011) estimate is as calculated in Howarth et al. (2012), using national emissions from EPA reports and national gas production data from US Department of Energy reports.

Table 2: Unconventional gas (shale gas and gas from tight sands), estimates of methane emissions from upstream (at the well site) plus midstream (at gas processing plants), expressed as the percentage of methane produced over the lifecycle of a well. Studies are listed chronologically by date of publication. Modified from Howarth et al., (2012)

Lagrangian Particle Dispersion modeling

Lagrangian Particle Dispersion Model
The tracer backward transport was simulated here by the Lagrangian Particle Dispersion Model (LPDM) described by Uliasz (1994). Particles are released from the receptors in a "backward in time" mode with the wind fields generated by the eulerian model WRF-FDDA. In a "backward in time" transport mode, particles are released in LPDM from the measurement locations and travel to the surface and the boundaries. Compared to a forward mode, all the particles here are used to estimate fluxes, which reduces the computational cost of the simulation. The Lagrangian model LPDM was enhanced to simulate aircraft observations based on the precise trajectory of the airplane estimated by GPS (Global Positioning System). At each second, 5 particles are released at the position of the aircraft. A longer integration time would yield more particles and hence more reliable Lagrangian statistics but would misrepresent the aircraft trajectory. We use higher resolution for the aircraft measurement period because the eventual particle distributions are more sensitive to the explicitly resolved vertical velocity.

Meteorological forcing
The dynamical fields in LPDM are forced by mean horizontal winds (u, v), potential temperature, and turbulent kinetic energy (TKE) from WRF-FDDA. At this resolution (1 km), turbulent motion corresponds to the closure of the energy budget at each time step. This scalar is used to quantify turbulent motion of particles as a pseudo random velocity. Based on the TKE, wind, and potential temperature, the Lagrangian model diagnoses turbulent vertical velocity and dissipation of turbulent energy. The off-line coupling between an Eulerian and a Lagrangian model solves most of the problems of non-linearity in the advection term at the mesoscale. Most of the non-linear processes resolved by the atmospheric model are attributed to a scalar representing the velocity of the particles. At each timestep (from one to 20 s), particles move with a velocity interpolated from the dynamical fields of the WRF-FDDA simulation (every 20 min). The timestep depends on the TKE, following the discretization described in Thomson (1987).

Source-Receptor relationship
The formalism for inferring source-receptor relationships from particle distributions is described by Seibert et al. (2004). At each time step, the fraction of particles (released from one receptor at one time) within some volume, gives the influence of that volume on the receptor. If the volume includes the surface this will yield the influence of surface sources. If the volume includes the boundary (sides or top) it yields the influence of that part of the boundary.

Deconvolution of CH_4 City emissions in the Barnett Shale aircraft campaign
The particles released during the segment of the flight (on March 27, 2013) corresponding to the enhancement of CH_4 mole fractions but not C_2H_6 mole fractions were selected as a test-case for the detection of CH_4 city signals. The three WRF simulations were coupled to the LPDM to generate footprints at the surface (Figure 8). These footprints were computed using the positions of the particles (gridded at 1km resolution) and compared to the spatial extent of the Dallas-Fort Worth urban area. In a perfect transport scenario, the spatial distribution of the particles at the surface should correspond to the urban area. We show here that:

- The WRF case (no FDDA – classic historical mode) shows that the footprints do not mach with the urban area, with an error in the wind direction,
- The WRF-FDDA case shows that the footprints are now aligned with the city limits, driven by a southern mean wind,
- The WRF-FDDA-aircraft case shows similar footprints as WRF-FDDA slightly shorter in the N-S direction.

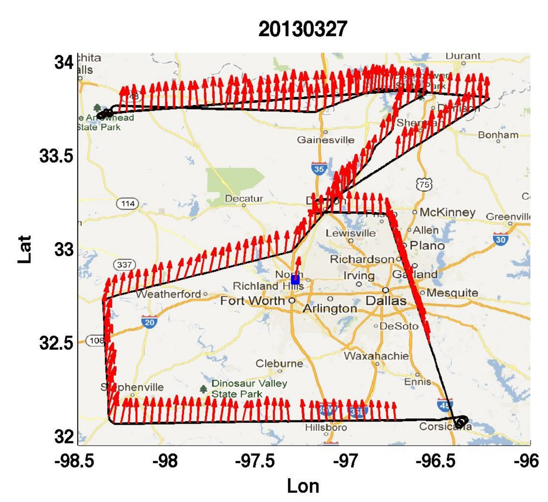

Figure 7: Map of wind vectors observed during the March 27, 2013 flight

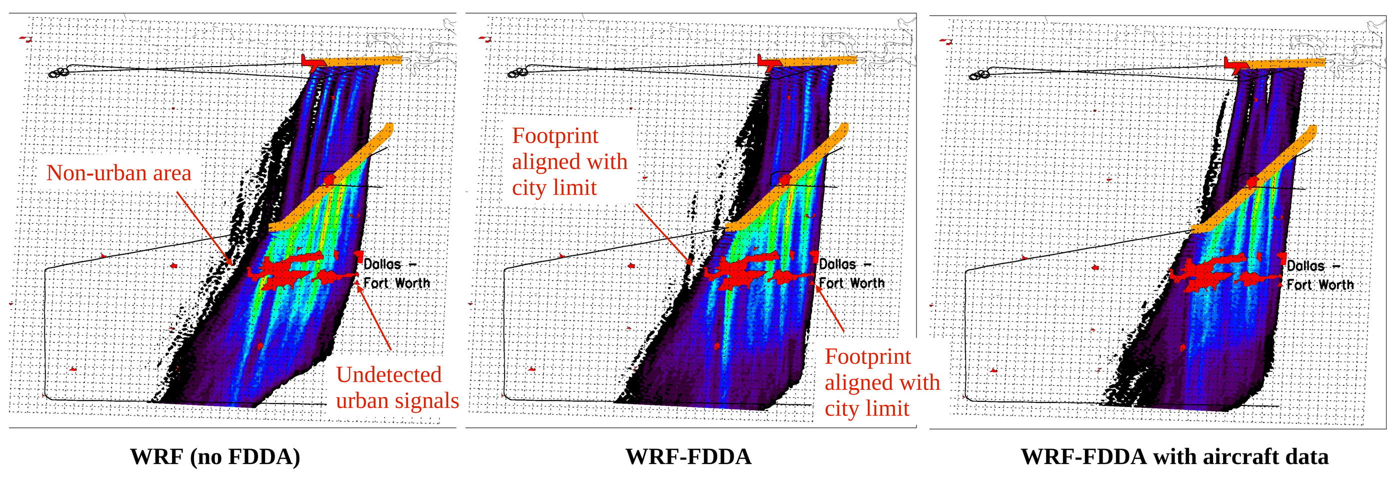

Figure 8: Concentration footprints (gridded at 1km resolution) based on the particle distributions using the LPDM (Uliasz, 1995) coupled to WRF (left panel), WRF-FDDA (middle panel), and WRF-FDDA with aircraft wind fields (right panel) corresponding to the low Ethane-to-methane ratio observed during the March 27 flight. Particles are released every second, and stored every minute.

References

Pétron, G., G. Frost, B. R. Miller, A. I. Hirsch, S. A. Montzka, A. Karion, M. Trainer, C. Sweeney, et al.: *Hydrocarbon emissions characterization in the Colorado Front Range: A pilot study, Journal of Geophysical Research-Atmospheres, 117, 2012.*

EPA/GRI (1996) Methane Emissions from the Natural Gas Industry. Prepared by Harrison, M., T. Shires, J. Wessels, and R. Cowgill, eds., Radian International LLC for National Risk Management Research Laboratory, Air Pollution Prevention and Control Division, Research Triangle Park, NC. EPA-600/R-96-080a.

Deng, A., D. Stauffer, B. Gaudet, J. Dudhia, J. Hacker, et al.: Update on WRF-ARW end-to-end multi-scale FDDA system. 10th Annual WRF Users' Workshop, 23 Jun 2009, Boulder, CO.

R. A. Alvarez, S. W. Pacala, J. J. Winebrake, W. L. Chameides, and S. P. Hamburg: Greater focus needed on methane leakage from natural gas infrastructure, PNAS, doi:10.1073/pnas.1202407109, 2012